ACADEMIC PRESS

Available online at www.sciencedirect.com
SCIENCE DIRECT®

Journal of Colloid and Interface Science 264 (2003) 517–525

JOURNAL OF Colloid and Interface Science

www.elsevier.com/locate/jcis

Boundary effect on the drag force on a nonhomogeneous floc

Jyh-Ping Hsu * and Yu-Heng Hsieh

Department of Chemical Engineering, National Taiwan University, Taipei, Taiwan 10617, Republic of China

Received 17 December 2002; accepted 5 May 2003

Abstract

The boundary effect on the drag force acting on a spherical floc having a nonhomogeneous structure is examined by considering a spherical floc at the centerline of a cylindrical tube. The floc is simulated by an entity having a two-layer structure, and its porous nature mimicked by varying the relative magnitude of the permeability of its inner and outer layers. The results of numerical simulation reveal that the tube wall has the effect of compressing the streamlines and vorticity contours. Also, as in the case of a rigid entity, the wake in the rear region of a floc, which arises from the convective motion of the fluid, is depressed. For fixed volume-averaged permeability, the influence of the tube wall on the behavior of a heterogeneous floc is more significant than that on the behavior of a homogeneous floc, and the influence varies with the structure of the former. The heterogeneous structure of a floc leads to a deviation in the modified drag coefficient–Reynolds number relation from a Stokes-law-like correlation. The smaller the average permeability of a floc the greater the deviation, but the presence of the tube wall has the effect of reducing the deviation.

Keywords: Spherical floc; Nonhomogeneous structure; Two-layer model; Boundary effect; Cylindrical tube; Drag force

1. Introduction

Boundary effects on the behavior of a moving entity in a dispersion medium play an important role in both fundamental theory and practical applications. The settling of flocs formed in typical wastewater treatment process, for example, involves evaluation of the hydrodynamic drag force on a floc, which is influenced both by the container wall and by neighboring flocs. The physical properties of floc are often estimated based on its terminal velocity in a settling tank. Apparently, the wall of the tank can play a role for flocs sufficiently close to it. Although relevant studies on the behavior of floc in a dispersion medium are ample in the literature, available results for the case where the boundary effect is significant are relatively limited. This include, for example, the movement of a rigid particle toward an impermeable plate, between two parallel plates, and along the centerline of a cylindrical tube, in the creeping flow regime [1]. Beyond the creeping flow regime, due to the convection motion of the dispersion medium, the streamlines at the front of a rigid particle can be asymmetric to those at its rear. In a study of the wall effect on the movement of an entity, Wham et al. [2] considered the case of a rigid sphere moving along the centerline of a circular tube for Reynolds number up to 100. They found that the presence of the tube wall has the effect of raising the drag force acting on the particle. Also, the Reynolds number for the onset of wake formation increases with the decrease in particle–wall distance, but the length of the wake decreases with this distance. Chhabra et al. [3] summarized the wall effect on the terminal velocity of a rigid sphere in a quiescent Newtonian fluid in a cylindrical tube for Reynolds number up to 200, and up to 3×10^5 when the wall effect is absent. Several attempts have been made to examine experimentally the wall effect on the behavior of a particle [4,5].

Floc formed in practice usually has an irregular shape, a highly porous and complicated, essentially random structure [6]. This is expected because floc usually comprises components with various characteristics, and the environments in which it is formed usually involve chaotic hydrodynamic conditions. The porous nature of floc was taken into account in the modeling of its behavior in a fluid medium by many investigators [7–12]. In a study of the behavior of a fractal aggregate with radially varying permeability in an infinite medium, Veerapaneni and Wiesner [13] proposed a multilayer model where a floc is divided into several shells each of which has a different permeability. A more concise

* Corresponding author.
E-mail address: jphsu@ccms.ntu.edu.tw (J.-P. Hsu).

0021-9797/$ – see front matter
doi:10.1016/S0021-9797(03)00506-X

two-layer model was used by Hsu and Hsieh [14] to simulate the behavior of a spherical floc in an infinite medium for the case of low to medium Reynolds number. Li and Ganczarczyk [15] examined experimentally the advective flow within an activated sludge floc, which comprised a permeable outer layer and an impermeable core. They showed that while small flocs are impermeable, flocs with size from 100 to 500 μm are permeable, in general, and the transport mechanism inside them is of advective nature [16]. Lee et al. [7] reported that the Reynolds number of the activated sludge floc obtained from a wastewater treatment plant of a bakery in a free-settling test ranged from 0.01 to 100, which implies that the classic Stokes law is inapplicable. Theoretical analyses based on a series of studies on the movement of a porous, homogeneous floc under various conditions also lead to the same conclusion [16–19].

As stated above, the structure of floc is of a complicated nature. In fact, inconsistent yet all realistic experimental observations have been reported in the literature. The experimental observation of Li and Ganczarczyk [6], for instance, revealed that the outer part of a floc is more compact than its inner part. In contrast, the outer part of the floc examined by Li and Ganczarczyk [20] was less compact than its inner part. These facts suggest that using a uniform model to simulate the behavior of a floc can be unrealistic, and a more general representation, which is capable of reflecting the nonuniform structure of a floc, is highly desirable. In this study, the boundary effect on the behavior of a nonrigid entity is examined by considering the movement of a porous, nonhomogeneous spherical floc along the axis of a cylinder for the case of low to medium Reynolds number. In particular, the drag force acting on a floc is estimated. The two-layer model proposed in our previous study [14] is adopted to simulate the nonuniform structure of a floc. This model is parsimonious in that the number of adjustable parameters is rather limited, but it is capable of simulating various structures of a floc by varying the relative magnitudes of the permeabilities of its inner and outer layers.

2. Theory

The problem under consideration is illustrated in Fig. 1, where a spherical floc of radius r_1 is placed on the axis of an infinite circular tube of radius R. The floc has a two-layer structure, and r_2 is the radius of its inner layer. The cylindrical coordinates (r, θ, z) are adopted with origin located at the center of the floc, r, θ, and z being respectively the dimensionless radial, the azimuthal, and the dimensionless axial coordinates, where r and z are scaled by r_1. The symmetric nature of the present problem suggests that only (r, z) coordinates need to be considered. Let (R, L) be the computation domain with $L \gg r_1$ and $L \gg R$. The floc moves with a constant velocity $-V$ along the z-axis, and the surrounding fluid is fixed. For convenience, we assume that the floc

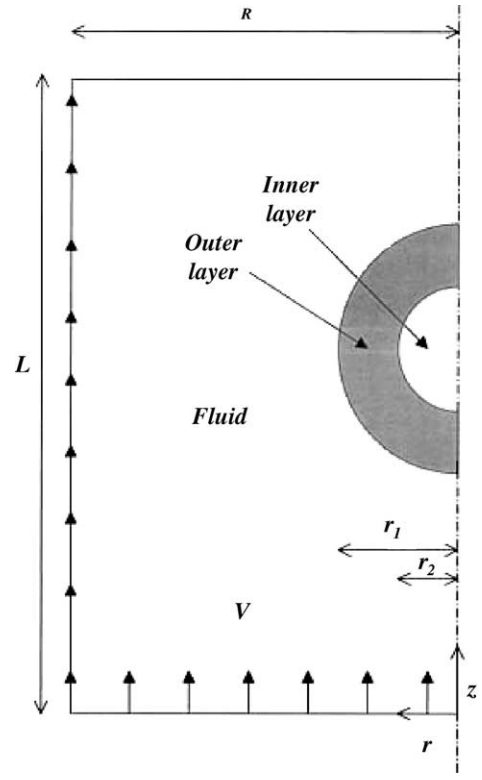

Fig. 1. Systematic representation of the problem considered. A spherical floc with a two-layer structure is placed on the axis of a cylinder of radius R filled with a Newtonian fluid. The radii of the outer and the inner layers of the floc are r_1 and r_2, respectively; r and z are respectively the radial and the axial coordinates, L is the computation domain in the axial coordinate, and $\boldsymbol{V}$ is the bulk velocity of the fluid.

remains fixed and the surrounding fluid flows with a constant bulk velocity $\boldsymbol{V}$.

We assume that the flow field in the liquid phase can be described by the Navier–Stokes equation [21] and the continuity equation. In dimensionless form, the former can be expressed as

$$\boldsymbol{u}_f \cdot \nabla \boldsymbol{u}_f = -\nabla P + \frac{2}{Re}\nabla^2 \boldsymbol{u}_f. \tag{1}$$

In cylindrical coordinates, we have, in the radial direction,

$$\left(\boldsymbol{u}_{f,r}\frac{\partial \boldsymbol{u}_{f,r}}{\partial r} + \boldsymbol{u}_{f,z}\frac{\partial \boldsymbol{u}_{f,r}}{\partial z}\right) = -\frac{\partial P}{\partial r} + \frac{2}{Re}\left(\frac{\partial}{\partial r}\left(\frac{1}{r}\frac{\partial}{\partial r}(r\boldsymbol{u}_{f,r})\right) + \frac{\partial^2 \boldsymbol{u}_{f,r}}{\partial z^2}\right), \tag{2}$$

and in the axial direction,

$$\left(\boldsymbol{u}_{f,r}\frac{\partial \boldsymbol{u}_{f,z}}{\partial r} + \boldsymbol{u}_{f,z}\frac{\partial \boldsymbol{u}_{f,z}}{\partial z}\right) = -\frac{\partial P}{\partial z} + \frac{2}{Re}\left(\frac{1}{r}\left(\frac{\partial}{\partial r}\left(r\frac{\partial \boldsymbol{u}_{f,z}}{\partial r}\right)\right) + \frac{\partial^2 \boldsymbol{u}_{f,z}}{\partial z^2}\right). \tag{3}$$

In dimensionless form, the continuity equation can be expressed as

$$\nabla \cdot \boldsymbol{u}_f = 0. \tag{4}$$

In cylindrical coordinates, we have

$$\frac{1}{r}\frac{\partial}{\partial r}(r\boldsymbol{u}_{f,r}) + \frac{\partial}{\partial z}(\boldsymbol{u}_{f,z}) = 0. \tag{5}$$

In these expressions, $Re = 2\rho r_1 V/\mu$ is the Reynolds number, ρ and μ are respectively the density and the viscosity of the fluid, r_1 and V are respectively the radius and the magnitude of $\boldsymbol{V}$, $P = (p + \rho g Z)/\rho V^2$ is the dimensionless modified pressure, p, g, and Z being respectively the pressure, the gravitational acceleration, and the vertical distance, ∇ is the dimensionless gradient operator scaled by $1/r_1$, $\boldsymbol{u}_f$ is the dimensionless fluid velocity scaled by V, and $\boldsymbol{u}_{f,r}$ and $\boldsymbol{u}_{f,z}$ are the radial and axial components of $\boldsymbol{u}_f$, respectively. We assume that the Darcy–Brinkman model [10] and the continuity equation are applicable to the description of the flow field inside a floc. In dimensionless form, the former can be expressed as

$$\boldsymbol{u}_i + \frac{Re}{2\beta_i^2}\nabla P = \nabla^2 \boldsymbol{u}_i. \tag{6}$$

In cylindrical coordinates, we have, in the radial direction,

$$\boldsymbol{u}_{i,r} + \frac{Re}{2\beta_i^2}\left(\frac{\partial P}{\partial r}\right) = \frac{\partial}{\partial r}\left(\frac{1}{r}\frac{\partial}{\partial r}(r\boldsymbol{u}_{i,r})\right) + \frac{\partial^2 \boldsymbol{u}_{i,r}}{\partial z^2}, \tag{7}$$

and in the axial direction,

$$\boldsymbol{u}_{i,z} + \frac{Re}{2\beta_i^2}\left(\frac{\partial P}{\partial z}\right) = \frac{1}{r}\left(\frac{\partial}{\partial r}\left(r\frac{\partial \boldsymbol{u}_{i,z}}{\partial r}\right)\right) + \frac{\partial^2 \boldsymbol{u}_{i,z}}{\partial z^2}. \tag{8}$$

In dimensionless form, the continuity equation for the flow field inside a floc is

$$\nabla \cdot \boldsymbol{u}_i = 0. \tag{9}$$

In cylindrical coordinates, we have

$$\frac{1}{r}\frac{\partial}{\partial r}(r\boldsymbol{u}_{i,r}) + \frac{\partial}{\partial z}(\boldsymbol{u}_{i,z}) = 0. \tag{10}$$

In these expressions, $\beta_i = r_1/\sqrt{k_i}$ is the scaled radius of a floc, k_i and $\boldsymbol{u}_i$ are respectively the permeability and the dimensionless velocity of the fluid in region i, and $i = 1$ and 2 represent respectively the outer and the inner layers of the floc. The dimensionless velocity is scaled by V, and $\boldsymbol{u}_{i,r}$ and $\boldsymbol{u}_{i,z}$ are the components of $\boldsymbol{u}_i$ in the radial and axial directions, respectively.

The following boundary conditions are assumed:

$$u_z = 1, \quad \text{on the wall of the tube,} \tag{11}$$

$$u_z = 1, \quad \text{as } z \to \infty, \tag{12}$$

$$\frac{\partial \boldsymbol{u}_f}{\partial r} = \frac{\partial \boldsymbol{u}_1}{\partial r} = \frac{\partial \boldsymbol{u}_2}{\partial r} = 0, \quad r = 0, \tag{13}$$

$$\boldsymbol{u}_f = \boldsymbol{u}_1 \quad \text{and the shear stress is continuous on the outer surface of outer layer,} \tag{14}$$

$$\boldsymbol{u}_1 = \boldsymbol{u}_2 \quad \text{and the shear stress is continuous on the outer surface of inner layer.} \tag{15}$$

In cylindrical coordinates Eq. (14) yields

$$\boldsymbol{u}_{f,r} = \boldsymbol{u}_{1,r} \quad \text{and} \quad \frac{\partial \boldsymbol{u}_{f,r}}{\partial r} = \frac{\partial \boldsymbol{u}_{1,r}}{\partial r}, \tag{16}$$

$$\boldsymbol{u}_{f,z} = \boldsymbol{u}_{1,z} \quad \text{and} \quad \frac{\partial \boldsymbol{u}_{f,z}}{\partial z} = \frac{\partial \boldsymbol{u}_{1,z}}{\partial z}, \tag{17}$$

and Eq. (15) gives

$$\boldsymbol{u}_{1,r} = \boldsymbol{u}_{2,r} \quad \text{and} \quad \frac{\partial \boldsymbol{u}_{1,r}}{\partial r} = \frac{\partial \boldsymbol{u}_{2,r}}{\partial r}, \tag{18}$$

$$\boldsymbol{u}_{1,z} = \boldsymbol{u}_{2,z} \quad \text{and} \quad \frac{\partial \boldsymbol{u}_{1,z}}{\partial z} = \frac{\partial \boldsymbol{u}_{2,z}}{\partial z}. \tag{19}$$

In these expressions $\boldsymbol{u}_z$ is the dimensionless fluid velocity in the z-direction and u_z is its magnitude.

The governing equations and the associated boundary conditions are solved numerically by FIDAP 8.6, which is a finite element scheme based on bilinear four-node quadrilateral elements. The numbers of elements chosen for the fluid domain and the outer and the inner layers of a floc are 18,800, 35, and 30, respectively.

3. Results and discussion

Extending the treatment of Neale et al. [10], we define

$$F = \left(\frac{1}{2}\rho V^2\right)(\pi r_1^2) C_D \Omega, \tag{20}$$

where F is the magnitude of the hydrodynamic drag force acting on a particle and C_D is the drag coefficient. The porous structure of the particle is taken into account by the correction factor Ω, $\Omega \leqslant 1$, and equality applies for a rigid particle. For the slow motion of a nonporous sphere C_D can be expressed as [21]

$$C_D = \frac{24}{Re}. \tag{21}$$

The analytic result of Neale et al. [10] for the slow motion of a porous floc in an infinite medium is adopted to justify the applicability of the numerical scheme adopted. It was found that the maximal percentage deviation in $C_D\Omega$ for all the cases examined is less than 0.1%.

The volume-averaged permeability of a floc, $\bar{k}$, and its volume-averaged radius, $\bar{\beta}$, are defined respectively by

$$\bar{k} = \sum_{i=1}^{2} V_i k_i \Big/ \sum_{i=1}^{2} V_i \tag{22}$$

and

$$\bar{\beta} = \frac{r_1}{\sqrt{\bar{k}}}. \tag{23}$$

Figure 2 shows the streamlines and the vorticity contours for various combinations of k_1/k_2 and r_1/R for the case where *Re* is small, and those for the case where *Re* is much larger are illustrated in Fig. 3. Note that because both r_1 and $\bar{\beta}$ are fixed in these figures, so is the volume-averaged

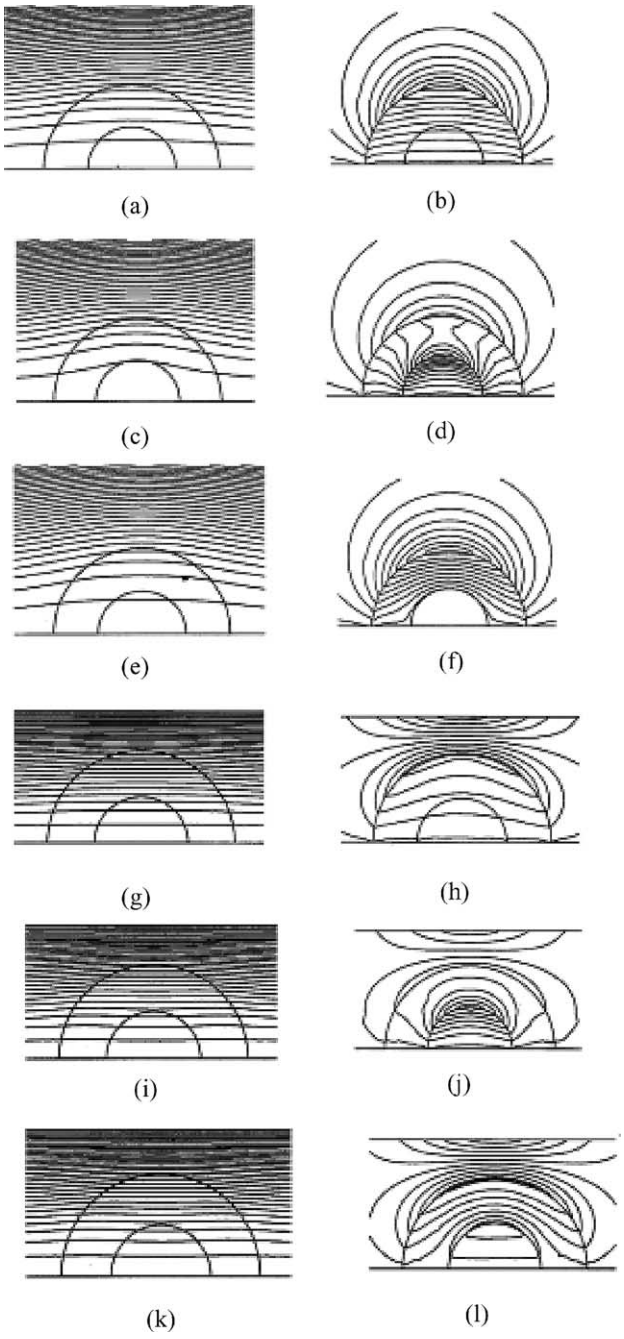

Fig. 2. Streamlines and vorticity contours at various k_1/k_2 for the case when $Re = 0.1$ and $\bar{\beta} = 2$. (a), (b) $k_1/k_2 = 1$ and $r_1/R = 0.1$; (c), (d) $k_1/k_2 = 10$ and $r_1/R = 0.1$; (e), (f) $k_1/k_2 = 0.1$ and $r_1/R = 0.1$; (g), (h) $k_1/k_2 = 1$ and $r_1/R = 0.7$; (i), (j) $k_1/k_2 = 10$ and $r_1/R = 0.7$; (k), (l) $k_1/k_2 = 0.1$ and $r_1/R = 0.7$. Key: $r_1 = 0.12$ cm, $\rho = 1$ g/cm^3, and $\mu = 0.01$ poise.

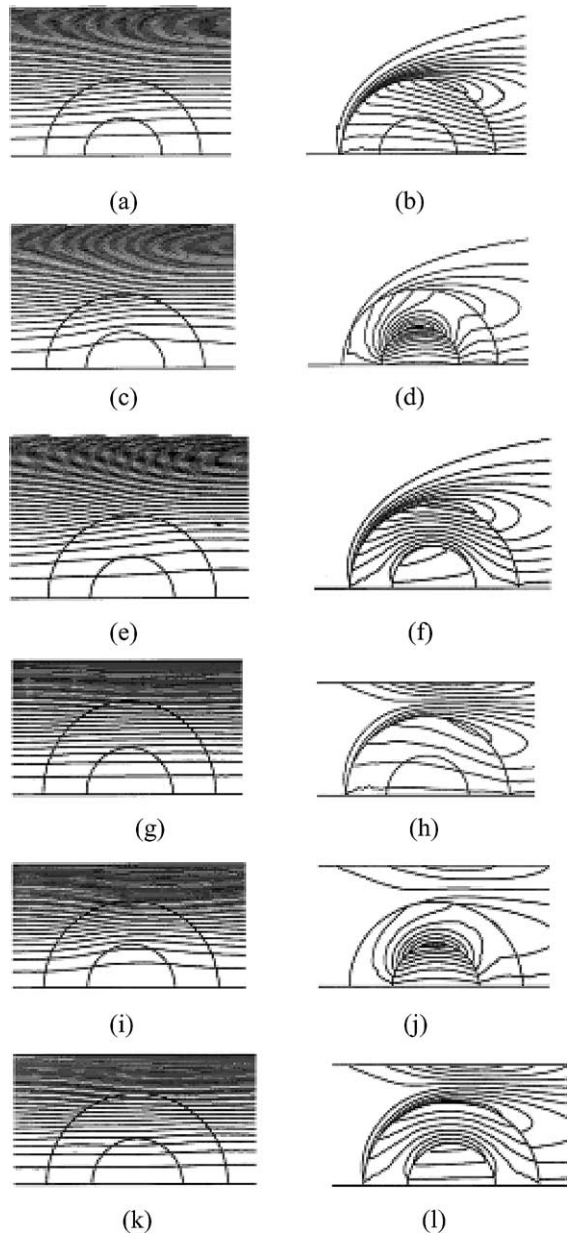

Fig. 3. Streamlines and vorticity contours at various k_1/k_2 as in Fig. 2 except that $Re = 40$.

permeability of a floc. In Figs. 2a, 2b, 2g, 2h, 3a, 3b, 3g, and 3h, $k_1/k_2 = 1$—i.e., a floc has a homogeneous structure; in Figs. 2c, 2d, 2i, 2j, 3c, 3d, 3i, and 3j, $k_1/k_2 = 10$—i.e., the inner layer of a floc is much less permeable than its outer layer; and in Figs. 2e, 2f, 2k, 2l, 3e, 3f, 3k, and 3l, the outer layer of a floc is much less permeable than its inner layer. Figures 2a–2f reveal that if *Re* is small, both the streamlines and the vorticity contours in the front region of a floc are symmetric to those in its rear region. The results shown in these figures are similar to that obtained by Hsu and Hsieh [13] for the case of an isolated floc. This is expected because r_1/R is small in Figs. 2a–2f; that is, the wall effect is relatively unimportant. Figures 2g–2l indicate that the presence of the tube wall has the effect of compressing the streamlines and the vorticity contours. The qualitative behavior of the streamlines and the vorticity contours for the case when $k_1/k_2 = 10$, illustrated in Fig. 2, are different from those for the case when $k_1/k_2 = 0.1$, even if the volume-averaged permeability is kept constant. This implies that the prediction of the flow field based on the mean property of a floc is unsatisfactory, and knowledge about its detailed structure is necessary. Figure 3 reveals that if *Re*

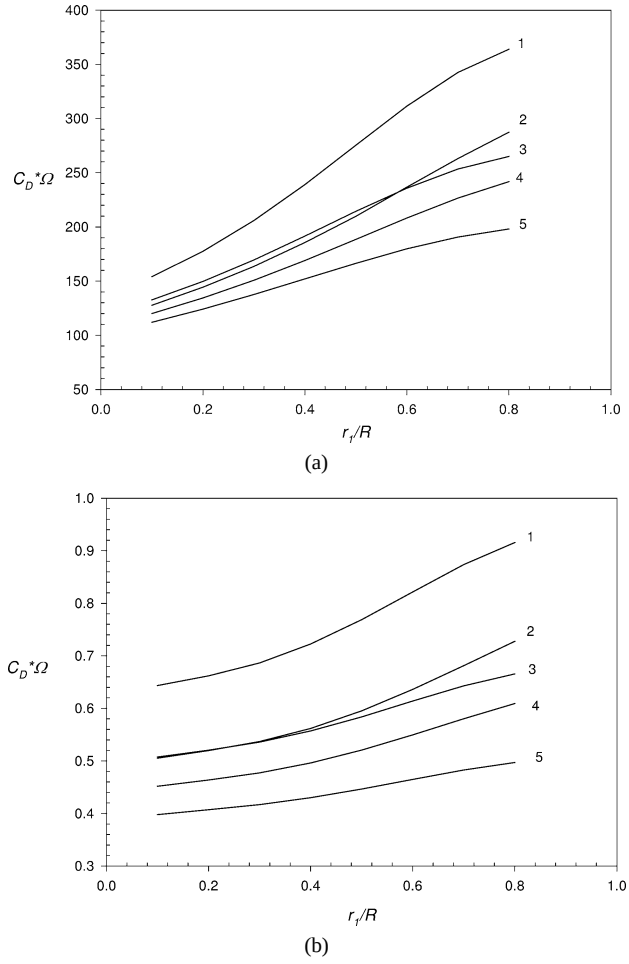

Fig. 4. Variation of $C_D\Omega$ as a function of r_1/R for various k_1/k_2 at two different *Re* for the case when $\bar{\beta} = 2$. Curve 1, $k_1/k_2 = 0.1$; 2, $k_1/k_2 = 0.2$; 3, $k_1/k_2 = 10$; 4, $k_1/k_2 = 5$; 5, $k_1/k_2 = 1$. (a) $Re = 0.1$, (b) $Re = 40$. Key: same as Fig. 2.

is sufficiently large, the convective motion of fluid becomes significant, as is justified by the observation that the streamlines and the vorticity contours in the front region of a floc are no longer symmetric to those in its rear region. Also, the presence of the tube wall has the effect of depressing the degree of asymmetry in streamlines and vorticity contours; that is, the convective motion of the fluid is compressed by the tube wall. Similar behavior was also observed for the case when a rigid particle is moving along the axis of a cylinder [21,22].

The variations of $C_D\Omega$ as a function of r_1/R for various k_1/k_2 at two different *Re* are presented in Fig. 4 for the case when $\bar{\beta}$ is fixed at 2. Here, the larger the r_1/R the closer a floc to the tube wall, and the more significant the boundary effect. In Fig. 4a, *Re* is small, and we have $[C_D\Omega(r_1/R = 0.8)/C_D\Omega(r_1/R = 0.1)] = 2.36$, 2.25, 2.00, 2.02, and 1.77 for $k_1/k_2 = 0.1$, 10, 0.2, 5, and 1, respectively. That is, for a fixed volume-averaged permeability, the effect of the wall on a homogeneous floc is less significant than that on a heterogeneous floc. Note that for the range of r_1/R examined, $C_D\Omega(k_1/k_2 = 1/10) > C_D\Omega(k_1/k_2 = 10)$, and $C_D\Omega(k_1/k_2 = 1/5) > C_D\Omega(k_1/k_2 = 5)$. That is, the effect of the wall on a floc with a less permeable outer layer (i.e., $k_1 = k_2/n$, n being an arbitrary constant larger than unity) is more important than that on a floc with a less permeable inner layer (i.e., $k_1 = nk_2$). This is because the outer part of a floc is closer to the wall than its inner part, and therefore, the effect of the former on $C_D\Omega$ is more important than that of the latter, even if the volume-averaged permeability is fixed. Note that in Fig. 4a, the curves corresponding to $k_1/k_2 = 1/5$ and $k_1/k_2 = 10$ intersect each other at a certain r_1/R; if r_1/R is small $C_D\Omega(k_1/k_2 = 1/5) > C_D\Omega(k_1/k_2 = 10)$, and the reverse is true if r_1/R is large. This implies that $C_D\Omega$ is influenced simultaneously by the structure of a floc and the degree of significance of the boundary effect. Figure 4a also indicates that, for a fixed average permeability, the influence of the boundary effect depends on the floc structure. For example, if $k_1/k_2 = 0.2$, $C_D\Omega$ increases from 132.65 to 264.97 as r_1/R varies from 0.1 to 0.8, and if $k_1/k_2 = 10$, it increases from 127.72 to 287.32. Figure 4b reveals that increasing the level of *Re* has the effect of reducing the significance of the boundary effect. For example, $[C_D\Omega(r_1/R = 0.8)/C_D\Omega(r_1/R = 0.1)] = 1.42$, 1.44, 1.31, 1.35, and 1.25 for $k_1/k_2 = 0.1$, 10, 0.2, 5, and 1, respectively. The calculation of $C_D\Omega$ at other values of $\bar{\beta}$ reveals that the boundary effect on a less permeable floc is more serious than that on a more permeable floc, which is consistent with the result of Wu and Lee [18]. For example, if $\bar{\beta} = 1$ and $Re = 0.1$, $[C_D\Omega(a/R = 0.8)/C_D\Omega(a/R = 0.1)] = 1.35$, 1.4, 1.25, 1.28, and 1.19 for $k_1/k_2 = 0.1$, 10, 0.2, 5, and 1, respectively. The qualitative behavior of $C_D\Omega$ as a/R and k_1/k_2 vary for the case when $Re = 0.1$ is similar to that when $Re = 40$, but the variation of $[C_D\Omega(r_1/R = 0.8)/C_D\Omega(r_1/R = 0.1)]$ as k_1/k_2 varies is less appreciable. We have, for $Re = 40$, $[C_D\Omega(r_1/R = 0.8)/C_D\Omega(r_1/R = 0.1)] = 1.12$, 1.16, 1.09, 1.11, and 1.08 for $k_1/k_2 = 0.1$, 10, 0.2, 5, and 1, respectively.

Figure 5 illustrates the variations of $C_D\Omega$ as a function of the scaled volume-averaged radius $\bar{\beta}$ for various k_1/k_2 at two different *Re*. Figure 5a reveals that at $Re = 0.1$, if $\bar{\beta}$ is small, the $C_D\Omega$ of a floc with $k_1/k_2 = 10$ (curve 1) is close to that with $k_1/k_2 = 0.1$ (curve 3); similarly, $C_D\Omega$ for $k_1/k_2 = 5$ (curve 2) is close to that for $k_1/k_2 = 1/5$ (curve 4). This implies that the $C_D\Omega$ of a highly permeable heterogeneous floc with $k_1 = 1/nk_2$ is about the same as that with $k_1 = nk_2$. However, the amount of increase in $C_D\Omega$ as $\bar{\beta}$ increases (or the volume-averaged permeability decreases) from 0.5 to 3 when $k_1/k_2 < 1$ is greater than that when $k_1/k_2 > 1$. That is, the $C_D\Omega$ of a highly porous floc is insensitive to its structure. Figure 5a also suggests that $C_D\Omega(k_1 = 1/nk_2) > C_D\Omega(k_1 = nk_2)$, which is consistent with the results shown in Fig. 4a. The qualitative behavior of $C_D\Omega$ for the case when $Re = 40$, shown in Fig. 5b, is similar to that when $Re = 0.1$, illustrated in Fig. 5a. Note that in the latter, curve 2 ($k_1/k_2 = 10$) intersects curve 3 ($k_1/k_2 = 0.2$) at a $\bar{\beta}$ smaller than 2, but curves 2 and 3 intersect at a $\bar{\beta}$ larger than 2 in the former.

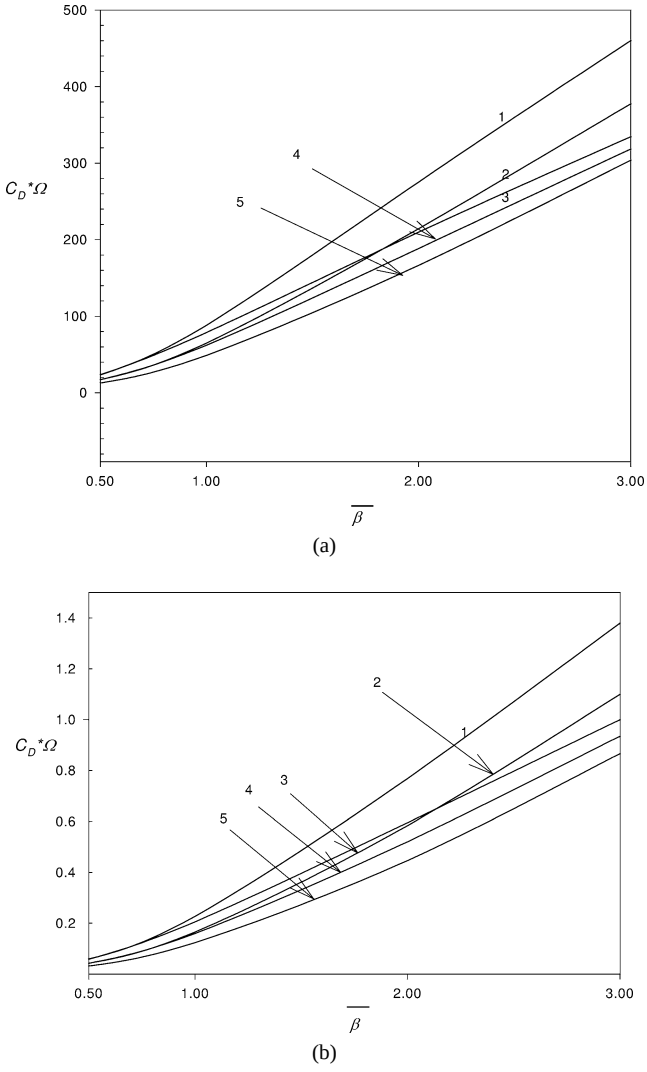

Fig. 5. Variation of $C_D\Omega$ as a function of $\bar{\beta}$ for various k_1/k_2 at two different Re for the case when $r_1/R = 0.5$. Curve 1, $k_1/k_2 = 0.1$; 2, $k_1/k_2 = 10$; 3, $k_1/k_2 = 0.2$; 4, $k_1/k_2 = 5$; 5, $k_1/k_2 = 1$. (a) $Re = 0.1$, (b) $Re = 40$. Key: same as Fig. 2.

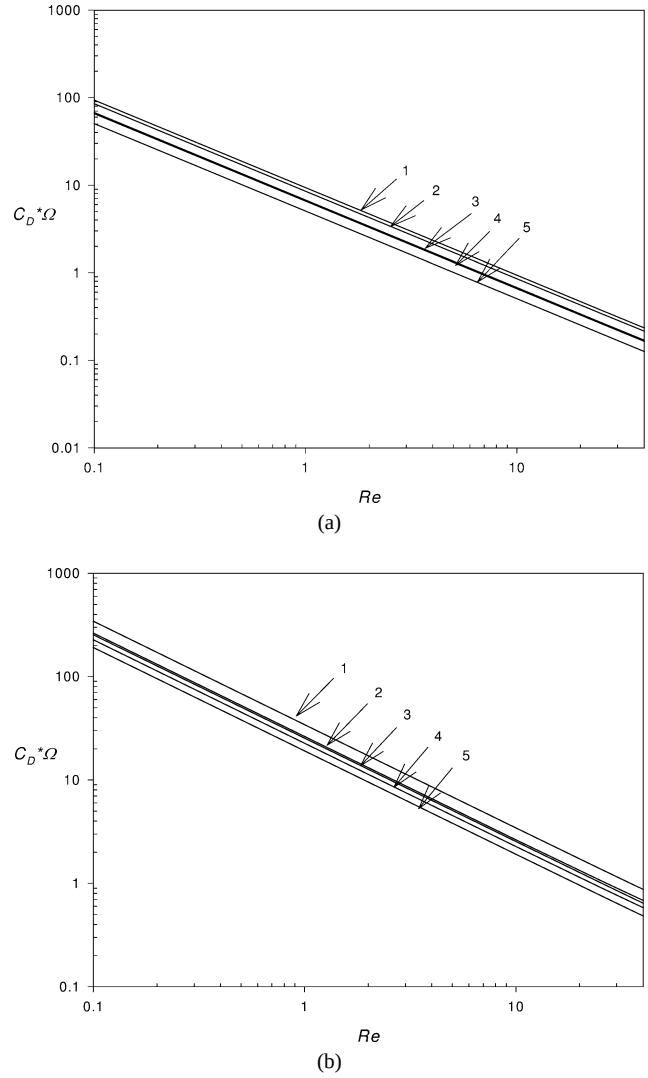

Fig. 6. Variation of $C_D\Omega$ as a function of Re for various k_1/k_2 at two different $\bar{\beta}$ for the case when $r_1/R = 0.7$. Curve 1, $k_1/k_2 = 0.1$; 2, $k_1/k_2 = 10$; 3, $k_1/k_2 = 0.2$; 4, $k_1/k_2 = 5$; 5, $k_1/k_2 = 1$. (a) $\bar{\beta} = 1$, (b) $\bar{\beta} = 2$. Key: same as Fig. 2.

For the present case, a Stokes-law-like correlation, which resembles Eq. (21), can be defined as

$$C_D\Omega = \frac{A(\bar{\beta}, k_1/k_2, r_1/R)}{Re}, \tag{24}$$

where A is a function of $\bar{\beta}$, k_1/k_2, and r_1/R. If this relation exists, then a plot of $\ln(C_D\Omega)$ against $\ln(Re)$ should give a straight line. In Fig. 6, $\ln(C_D\Omega)$ is plotted against $\ln(Re)$ for various k_1/k_2 at two different $\bar{\beta}$ for the case $r_1/R = 0.7$. This figure reveals that while $\ln(C_D\Omega)$ and $\ln(Re)$ are roughly linearly correlated when Re is small, some positive deviation from the linear relation is observed when Re is large. This deviation depends on the magnitude of $\bar{\beta}$. For example, at $Re = 40$ the deviations of $C_D\Omega$ of a floc with $k_1/k_2 = 0.1$, 10, 0.2, 5, and 1 from the Stokes-law-like relation, Eq. (24), when $\bar{\beta} = 1$ are all smaller than 1%, and they are 2%, 3.6%, 1.5%, 2.5%, and 1.3%, respectively, when $\bar{\beta} = 2$. The deviation from the Stokes-law-like relation depends also on the magnitude of r_1/R; the smaller the r_1/R the more serious the deviation is. For example, at $r_1/R = 0.1$ the deviations from the Stokes-law-like relation are 20.6%, 21.7%, 14.5%, 15.7%, and 10.5%, respectively, when $\bar{\beta} = 1$, and are 67.1%, 53%, 58.2%, 50.6%, and 42%, respectively, when $\bar{\beta} = 2$. Therefore, we conclude that if the boundary effect is relatively unimportant, the more heterogeneous a floc, and/or the larger the $\bar{\beta}$ is, the greater the deviation of $C_D\Omega$ from the corresponding Stokes-law-like relation, and the presence of the tube wall has the effect of reducing this deviation.

The variations of the $C_D\Omega$ of a floc as a function of k_1/k_2 for various combinations of Re and r_1/R are illustrated in Fig. 7. Figure 7a indicates that if $r_1/R = 0.1$ and $Re = 0.1$, $C_D\Omega(k_1/k_2 = 0.01) = 4.23C_D\Omega(k_1/k_2 = 1)$ and $C_D\Omega(k_1/k_2 = 100) = 2.55C_D\Omega(k_1/k_2 = 1)$; that is,

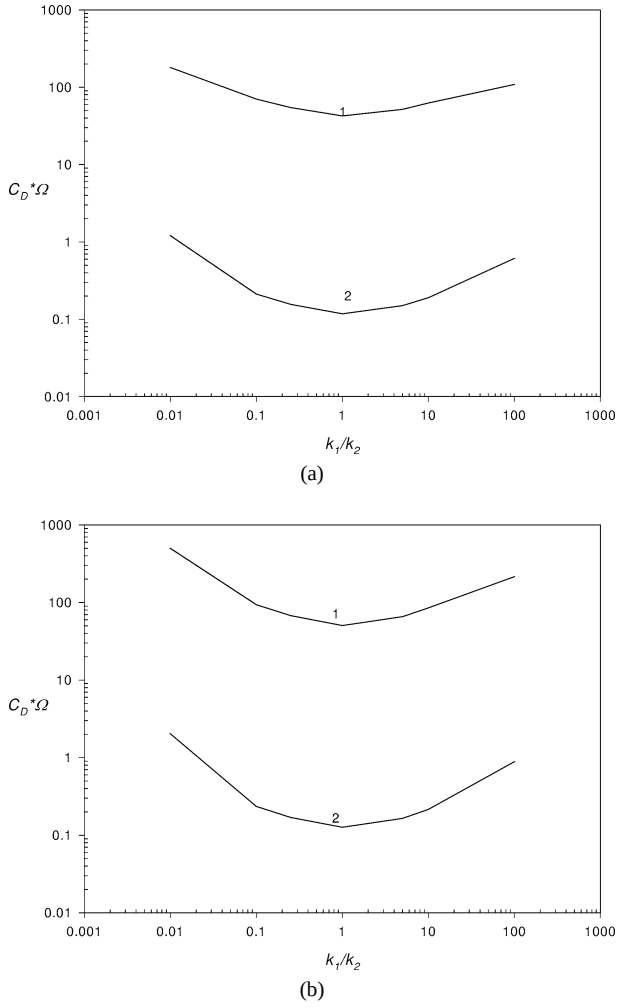

Fig. 7. Variation of $C_D\Omega$ as a function of k_1/k_2 at various combinations of Re and r_1/R for the case when $\bar{\beta} = 1$. Curve 1, $Re = 0.1$; 2, $Re = 40$. (a) $r_1/R = 0.1$, (b) $r_1/R = 0.7$. Key: same as Fig. 2.

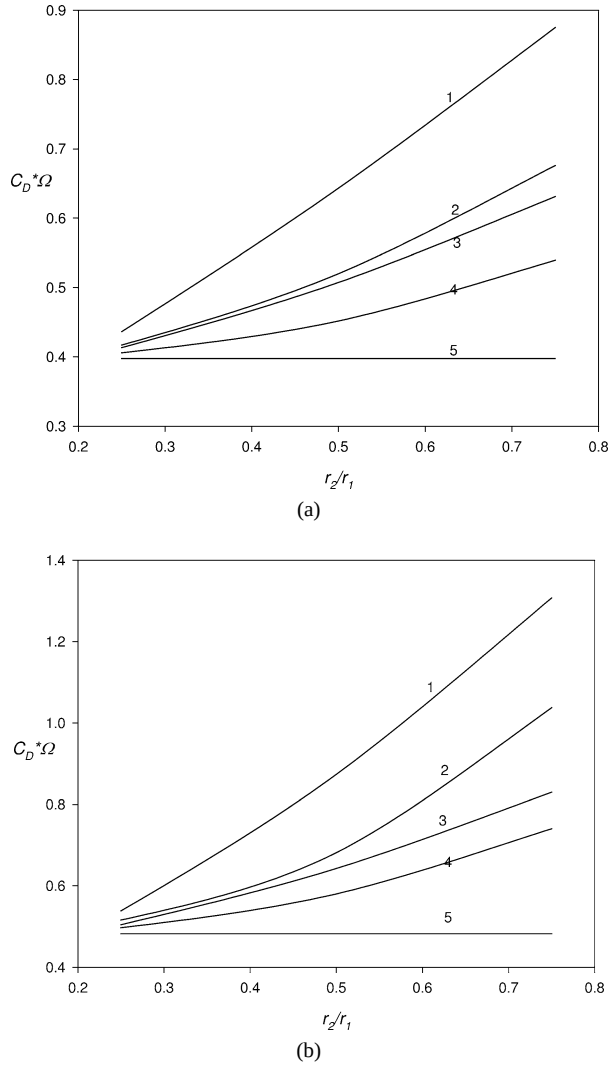

Fig. 8. Variation of $C_D\Omega$ as a function of r_2/r_1 for various k_1/k_2 at two different r_1/R for the case when $\bar{\beta} = 2$ and $Re = 40$. Curve 1, $k_1/k_2 = 0.1$; 2, $k_1/k_2 = 10$; 3, $k_1/k_2 = 0.2$; 4, $k_1/k_2 = 5$; 5, $k_1/k_2 = 1$. (a) $r_1/R = 0.1$, (b) $r_1/R = 0.7$. Key: same as Fig. 2.

$C_D\Omega(k_1/k_2 = 0.01) > C_D\Omega(k_1/k_2 = 100)$. As discussed previously, this is because the boundary effect for the case when $k_1 = nk_2$ is different from that for the case when $k_1 = 1/nk_2$. If $r_1/R = 0.1$ and $Re = 40$, we have $C_D\Omega(k_1/k_2 = 0.01) = 4C_D\Omega(k_1/k_2 = 1)$ and $C_D\Omega(k_1/k_2 = 100) = 2.02C_D\Omega(k_1/k_2 = 1)$. The qualitative behavior of $C_D\Omega$ presented in Fig. 7b is similar to that illustrated in Fig. 7a. If $r_1/R = 0.7$ and $Re = 0.1$, we have $C_D\Omega(k_1/k_2 = 0.01) = 9.9C_D\Omega(k_1/k_2 = 1)$ and $C_D\Omega(k_1/k_2 = 100) = 4.27C_D\Omega(k_1/k_2 = 1)$, and if $r_1/R = 0.7$ and $Re = 40$, we have $C_D\Omega(k_1/k_2 = 0.01) = 6.29C_D\Omega(k_1/k_2 = 1)$ and $C_D\Omega(k_1/k_2 = 100) = 2.74C_D\Omega(k_1/k_2 = 1)$. We conclude from Fig. 7 that for both $Re = 0.1$ and $Re = 40$, the presence of the tube wall has the effect of increasing the value of $C_D\Omega$, which arises from the heterogeneous structure of a floc.

Figure 8 shows the variation of $C_D\Omega$ as a function of the ratio (radius of inner layer/radius of floc), r_2/r_1, at two different r_1/R for the case when $Re = 40$. Note that the curve 5 in both Figs. 8a and 8b is horizontal because it represents the result for a homogeneous floc. As can be seen in Fig. 8a, if $k_1/k_2 \neq 1$, $C_D\Omega$ increases with the increase in r_2/r_1. In particular, if $r_1/R = 0.1$, we have $C_D\Omega(k_1/k_2 = 0.1, r_2/r_1 = 0.75) = 2C_D\Omega(k_1/k_2 = 0.1, r_2/r_1 = 0.25)$, $C_D\Omega(k_1/k_2 = 10, r_2/r_1 = 0.75) = 1.62C_D\Omega(k_1/k_2 = 10, r_2/r_1 = 0.25)$, $C_D\Omega(k_1/k_2 = 0.2, r_2/r_1 = 0.75) = 1.53C_D\Omega(k_1/k_2 = 0.2, r_2/r_1 = 0.25)$, $C_D\Omega(k_1/k_2 = 5, r_2/r_1 = 0.75) = 1.33C_D\Omega(k_1/k_2 = 5, r_2/r_1 = 0.25)$. Note that if $k_1/k_2 < 1$, the outer layer of a floc become less permeable as r_2/r_1 increases, which yields a larger $C_D\Omega$. On the other hand, if $k_1/k_2 > 1$, the less permeable inner layer of a floc is closer to tube wall as r_2/r_1 increases, which also yields a larger $C_D\Omega$. The qualitative behavior of $C_D\Omega$ presented in Fig. 8b for the case when r_1/R is large is similar to that shown in Fig. 8a for the case when r_1/R is small. The degree of increase in $C_D\Omega$ as r_2/r_1 increases is enhanced by the presence of the tube wall. For example, at $r_1/R = 0.7$, $C_D\Omega(k_1/k_2 = 0.1, r_2/r_1 = 0.75) = 2.43C_D\Omega(k_1/k_2 =$

$0.1, r_2/r_1 = 0.25)$, $C_D\Omega(k_1/k_2 = 10, r_2/r_1 = 0.75) = 2.06C_D\Omega(k_1/k_2 = 0.2, r_2/r_1 = 0.25)$, $C_D\Omega(k_1/k_2 = 0.2, r_2/r_1 = 0.75) = 1.65C_D\Omega(k_1/k_2 = 10, r_2/r_1 = 0.25)$, and $C_D\Omega(k_1/k_2 = 5, r_2/r_1 = 0.75) = 1.49C_D\Omega(k_1/k_2 = 5, r_2/r_1 = 0.25)$. Figure 8 indicates that for a fixed volume-averaged permeability, $C_D\Omega$ increases with the increase in the size of the inner layer of a floc, in general.

In summary, the wall effect on the drag force experienced by a nonuniformly structured spherical floc on the axis of a cylinder tube filled with a Newtonian fluid is evaluated based on a two-layer model. The result of numerical simulation reveals the followings:

(i) The presence of the tube wall has the effect of compressing the streamlines, the vorticity contours, and the wake in the rear part of the floc, which arises from the convective motion of the fluid.
(ii) For a fixed volume-averaged permeability, the influence of the tube wall on the behavior of a floc depends upon its structure; the influence on a heterogeneous floc is more significant than that on a homogeneous floc.
(iii) The heterogeneous structure of a floc leads to a deviation in the (drag coefficient × correction factor) from a Stokes-law-like relation. The larger the scaled radius of a floc the greater the deviation, and the more significant the boundary effect the smaller the deviation.
(iv) Regardless of the magnitude of Reynolds number, the presence of tube wall has the effect of increasing the drag force, which arises from the heterogeneous structure of a floc.

Acknowledgment

This work is supported by the National Science Council of the Republic of China.

Appendix A. Nomenclature

A	function of $\bar{\beta}$, k_1/k_2, and r_1/R, dimensionless
C_D	drag coefficient, dimensionless
$\boldsymbol{F}$	hydrodynamic drag force (N)
F	magnitude of $\boldsymbol{F}$ (N)
g	gravitational acceleration (m/s^2)
$\bar{k}$	volume-averaged permeability (m^2)
k_1	permeability of the outer layer of a floc (m^2)
k_2	permeability of the inner layer of a floc (m^2)
L	computational domain in axial direction (m)
n	positive constant, dimensionless
p	pressure (N/m^2)
P	scaled modified pressure, dimensionless
R	radius of circular tube or computational domain in radial direction (m)
Re	Reynolds number, dimensionless
r	scaled radial coordinate, dimensionless
r_1	radius of floc (m)
r_2	radius of inner layer of a floc (m)
$\boldsymbol{u}_f$	scaled fluid velocity in fluid domain, dimensionless
u_f	magnitude of $\boldsymbol{u}_f$, dimensionless
$\boldsymbol{u}_{f,r}$	scaled fluid velocity in radial direction in fluid domain, dimensionless
$\boldsymbol{u}_{f,z}$	scaled fluid velocity in axial direction in fluid domain, dimensionless
$\boldsymbol{u}_1$	scaled fluid velocity in the outer layer of a floc, dimensionless
u_1	magnitude of $\boldsymbol{u}_1$, dimensionless
$\boldsymbol{u}_2$	scaled fluid velocity in the inner layer of a floc, dimensionless
u_2	scaled magnitude of $\boldsymbol{u}_2$, dimensionless
$\boldsymbol{u}_{i,r}$	scaled fluid velocity in radial direction in floc domain i, dimensionless
$\boldsymbol{u}_{i,z}$	scaled fluid velocity in axial direction in floc domain i, dimensionless
$\boldsymbol{u}_z$	scaled fluid velocity along z-axis, dimensionless
$\boldsymbol{V}$	floc velocity (m/s)
V	magnitude of $\boldsymbol{V}$ (m/s)
z	scaled axial coordinate, dimensionless
Z	vertical distance (m)

Greek letters

β_i	scaled radius of floc, dimensionless
$\bar{\beta}$	scaled volume-averaged radius of floc, dimensionless
μ	viscosity of fluid (Pa s)
ρ	density of fluid (kg/m^3)
θ	azimuthal coordinates (radian)
∇	scaled gradient operator, dimensionless
Ω	correction factor, dimensionless

References

[1] J. Happel, H. Brenner, Low Reynolds Number Hydrodynamics, Academic Press, New York, 1983.
[2] R.M. Wham, O.A. Basaran, C.H. Byers, Ind. Eng. Chem. Res. 35 (1996) 864.
[3] R.P. Chhabra, S. Agarwal, K. Chaudhary, Powder Technol. 129 (2003) 53.
[4] R.P. Chhabra, Powder Technol. 85 (1995) 83.
[5] R. Di Felice, L.G. Gibilaro, P.U. Foscolo, Chem. Eng. Sci. 50 (1995) 3005.
[6] D.H. Li, J. Ganczarczyk, Biotechnol. Bioeng. 35 (1990) 57.
[7] D.J. Lee, G.W. Chen, Y.C. Liao, C.C. Hsieh, Water Res. 30 (1996) 541.
[8] P.M. Alder, J. Colloid Interface Sci. 81 (1981) 531.
[9] A.C. Pyatakes, D. George, Chem. Eng. Sci. 58 (1987) 119.
[10] G. Neale, N. Epstein, W. Nader, Chem. Eng. Sci. 28 (1973) 1865.
[11] T.N. Smith, Chem. Eng. Sci. 53 (1998) 315.
[12] K. Matsumoto, A. Suganuma, Chem. Eng. Sci. 32 (1977) 445.
[13] S. Veerapaneni, M.R. Wiesner, J. Colloid Interface Sci. 177 (1996) 45.
[14] J.P. Hsu, Y.H. Hsieh, Chem. Eng. Sci. 57 (2002) 2627.
[15] D.H. Li, J. Ganczarczyk, Water Environ. Res. 64 (1992) 236.
[16] R.M. Wu, D.J. Lee, Water Res. 32 (1998) 760.

[17] R.M. Wu, D.J. Lee, Chem. Eng. Sci. 53 (1998) 3571.
[18] R.M. Wu, D.J. Lee, Chem. Eng. Sci. 54 (1999) 5717.
[19] R.M. Wu, D.J. Lee, Water Res. 35 (2001) 3226.
[20] D.H. Li, J. Ganczarczyk, Water Res. 22 (1988) 789.
[21] R.B. Bird, W.E. Stewart, E.N. Lightfoot (Eds.), Transport Phenomena, Wiley, New York, 1960.
[22] R. Clift, J. Grace, M.E. Weber (Eds.), Bubbles, Drops and Particles, Academic Press, New York, 1978.